Earth and Planetary Science Letters 503 (2018) 248–251

Contents lists available at ScienceDirect

Earth and Planetary Science Letters

www.elsevier.com/locate/epsl

Comment on “Late Miocene–Pliocene Asian monsoon intensification linked to Antarctic ice-sheet growth” [Earth Planet. Sci. Lett. 444 (2016) 75–87]

Rui Zhang [a,b,c], Vadim A. Kravchinsky [a,b,*], Taslima Anwar [b], Leping Yue [a,c], Jianxing Li [c,a], Jin Jiao [a]

[a] *Institute of Cenozoic Geology and Environment, State Key Laboratory of Continental Dynamics, Department of Geology, Northwest University, Xi’an 710069, China*

[b] *Geophysics, Department of Physics, University of Alberta, Edmonton, Alberta T6G 2E1, Canada*

[c] *Xi’an Center of Geological Survey, China Geological Survey, Xi’an 710054, China*

ARTICLE INFO

Article history:
Received 19 February 2018
Accepted 16 August 2018
Editor: B. Buffett

Eolian sediment sequences on the Chinese Loess Plateau (CLP) are one of the best continental archives of paleoclimate change in the late Cenozoic Era. Variations in paleoclimate proxies in loess sequences, such as magnetic susceptibility (MS) and sedimentary grain size (GS), are standard tools to evaluate the time series of paleoclimatic fluctuations that bear a remarkable correlation with monsoon variability on multimillennial timescales. Monsoonal dynamics are linked to the rhythms of solar insolation, ice volume changes, and ocean–atmosphere energy exchange (Ding et al., 1994).

Recently, Ao et al. (2016) published an 8 Myr record of the enhanced Miocene–Pliocene monsoon intensification model linked to the stepwise increase of the Antarctic ice-sheet. Their climate change evaluation is based on the age model of the so-called New Shilou red clay section situated ∼13 km southeast of Shilou County (Shanxi Province) on the eastern CLP. The New Shilou section is situated ∼1 km from the Shilou section, which was already dated at 11 Myr using magnetostratography (Xu et al., 2009). In 2015, T.A., V.A.K., and R.Z. re-examined the magnetostratigraphic, MS and GS data for the Shilou section applying the analysis of orbital periodicities registered in the climate proxies (Anwar et al., 2015). After creating a first-order magnetostratigraphic correlation with the geomagnetic polarity time scale (GPTS), Anwar et al. (2015) performed spectral analysis of the MS and GS time series. If the spectral peaks of the MS and GS data sets did not correspond to any Milankovitch periodicities, they found a new correlation between the geomagnetic polarity record in the section and the GPTS and created another new age model. The iterative procedure was repeated until the 400 and 100 kyr eccentricity cycles showed the best resolution. Once the eccentricity cycles were confidently resolved, the correlation of the geomagnetic polarity pattern with the GPTS was considered to be confirmed and the final magnetostratigraphic age model was produced. The sedimentation rates in the section were continuously monitored during every iterative step to avoid any sudden unexplained rate jumps in the section. After the final age model was established, the section was dated at 5.2 Ma, which is cardinally different from the age models in Xu et al. (2009, 2012) and Ao et al. (2016). Anwar et al. (2015) pointed out that magnetostratigraphy dating based only on visual correlation could potentially lead to an erroneous age model, as some of the polarity events could be misinterpreted. Anwar et al. (2015) assessed the paleomonsoon evolution only after establishing a reliable age model.

This comment points to two major oversights in Ao et al. (2016) that could lead to an erroneous age model and consequently to incorrect paleoclimate interpretation. (1) A subjective visual correlation of the red clay magnetostratigraphic profile with the GPTS provided in Xu et al. (2009) and Ao et al. (2016) cannot produce a reliable age model without a cyclostratigraphic approach, especially in the absence of biostratigraphy or isotope stratigraphy constraints. (2) High-resolution continuous sampling enables

DOI of original article: https://doi.org/10.1016/j.epsl.2016.03.028.
DOI of reply to comment: https://doi.org/10.1016/j.epsl.2018.08.045.

* Corresponding author at: Geophysics, Department of Physics, University of Alberta, Edmonton, Alberta T6G 2E1, Canada.
E-mail address: vadim@ualberta.ca (V.A. Kravchinsky).

https://doi.org/10.1016/j.epsl.2018.08.033

the resolution not only of geomagnetic polarity zones but also of short geomagnetic events, geomagnetic excursions in environments with relatively high sedimentation rates. Special precautions must be taken when correlating the magnetostratigraphic section to the GPTS to avoid defining a geomagnetic excursion as a geomagnetic polarity event. Cande and Kent (1992) applied an arbitrary cut-off of polarity events shorter than 30 kyr from the GPTS in order to separate geomagnetic polarity reversals from geomagnetic anomalies due to short-term variations. Thus, the GPTS is a smoothed record that excludes geomagnetic excursions and so-called tiny wiggles. The principle is adapted in all GPTS versions (Cande and Kent, 1995; Gee and Kent, 2007; Ogg, 2012). Direct correlation of every polarity event in the red clay sections to every GPTS polarity chron would potentially lead to an erroneous age model if there is no additional age evidence (fossils, absolute dating, or cyclostratigraphy).

Magnetostratigraphy of red clay successions in central and eastern parts of the CLP have been established in many sections by visual correlation between geomagnetic events and the GPTS (Supplementary Fig. 1). Supplementary Table 1 summarizes thickness and sedimentation rates of the major red clay sections on the central and eastern CLP. Some of these sections contain classical loess sections on top of the red clay. Based on different age models produced by visual correlation with the GPTS, published red clay sections can be divided into two groups based on sedimentation rate (Supplementary Table 1), that is, high sedimentation rates of 22–28 mm/kyr and low sedimentation rates of 11–14 mm/kyr. However, grain size and magnetic susceptibility in these red clay sequences show only slight variations from north to south (Ding et al., 2000). Anwar's age model placed the Shilou section into the high sedimentation rate group whereas age models in Xu et al. (2009) and Ao et al. (2016) and more recent Ao et al. (2017) placed the Shilou section into the low sedimentation rate group based on visual correlation (Supplementary Table 1).

Only a few studies performed a spectral analysis of the MS data to confirm the correctness of their magnetostratigraphic age models for red clay with Milankovitch periodicities (Evans et al., 1991; Vandenberghe et al., 2004; Sun et al., 2006, 2010; Nie, 2011). Eccentricity cycles of 400 and 100 kyr were reported to be 2.6–3.4 Ma for Lingtai (Sun et al., 2006) and 2–4 Ma for Chaona (Nie, 2011) and Baoji (Evans et al., 1991). In Supplementary Table 1, red clay sections where spectral analysis was performed to evaluate Milankovitch periodicities are placed in the group with high sedimentation rates, that is, Lingtai (Sun et al., 2006), Chaona (Nie, 2011), and Shilou (Anwar et al., 2015). An exception is the very first magnetostratigraphic work on red clay in the Baoji section (Evans et al., 1991). Evans et al. (1991) discussed a possible drawback of their time scale and the possibility of an alternative age model for the Baoji section.

Ao et al. (2016) incorrectly referred to a micromammal fossil in the nearest Shilou section (Xu et al., 2012) to support their visual correlation of the geomagnetic polarity pattern in the New Shilou section with the GPTS. Xu et al. (2012) did not describe any micromammal findings, but mentioned a single tooth finding in their section. It must be noted that the tooth was dated using their magnetistratigraphic age model, it was not the date of the tooth that contributed to the age model (Xu et al., 2012). Moreover, Xu et al. (2012) clearly stated that there were no large mammal fossils in the section. Therefore, the tooth finding cannot be used as evidence to support the magnetostratigraphic age model of Ao et al. (2016). In short there are no biostratigraphic constraints in either the Shilou or the New Shilou section.

Assigning a magnetostratigraphy interval as a polarity chron or a geomagnenetic excursion is a challenging task and a subjective approach could lead to erroneous interpretation in red clay sequences without independent age controls. In the same section, sedimentation rates are variable for different time intervals and the deposition process is not perfectly continuous in eolian sequences (Zhu et al., 2007). These factors can lead to a situation in which a geomagnetic excursion could be interpreted as a longer polarity interval and a polarity chron could appear to be a short geomagnetic event. In Ao et al. (2016) some polarity intervals are mistakenly interpreted as geomagnetic excursions and vice versa, while polarity intervals and geomagnetic excursions still correlate with polarity subchrons on the GPTS. In Fig. 1 we reanalyze the correlation of polarity intervals and geomagnetic excursions with the GPTS and compare the polarity intervals and geomagnetic excursions with the age model in Anwar et al. (2015). Seven polarity intervals are discussed below.

The average sedimentation rates are 26 mm/kyr for the Shilou section (Anwar et al., 2015) and 16 mm/kyr for the New Shilou section (Ao et al., 2016), therefore, thicknesses of <0.78 m in the Shilou section and <0.48 m in the New Shilou section correspond to a time interval of ≤ 30 kyr. Short polarity records from the profile in Ao et al. (2016) with ≤ 30 kyr duration should therefore be considered to be geomagnetic excursions not registered in the standard GPTS. Ao et al. (2016) considered every polarity event to be a GPTS interval. However, Spassov et al. (2011) numerically modeled their record of the Olduvai subchron termination in the Lingtai section and concluded that the loess does not necessarily represent an actual transitional polarity change interval but reflects lithogenic variations. Jin et al. (2012) demonstrated that only a statistical approach can effectively evaluate the presence of short polarity events of a few thousand years duration with a condition that the event is already firmly dated. They effectively evaluated a geomagnetic precursor to the Matuyama–Brunhes reversal in Chinese loess using five sets of direction data. This implies that visual correlation of short geomagnetic events to the GPTS can produce an erroneous age model, as demonstrated by Anwar et al. (2015).

Further, we re-evaluated the magnetostratigraphic profile from Ao et al. (2016) by removing eight suspected short geomagnetic events from the correlation with the GPTS. After this procedure the profile becomes identical to the profile in Anwar et al. (2015) (Fig. 1). Ao et al. (2016) ignored short event 1, which was represented by only 2 samples ($\sim$0.4 m, i.e., ≤ 30 kyr), however, interpreting comparable thickness events 6 (4 samples) and 7 (2 samples) as polarity chrons. Short event 2 is about 1 m thick, representing a time interval of about 80 kyr, but short event 3 is only $\sim$30–40 kyr long, however, it is correlated to the 100 kyr long polarity interval of 3.2–3.3 Ma in the GPTS (Ao et al., 2016). Besides, event 3 does not have fully reversed directions; the inclinations barely pass into negative numbers. Three negative inclination excursions are reported in the normal polarity interval C2An.n1 in the Lake Baikal record (Kravchinsky, 2017) and four excursions are reported in oceanic sediments (Ohno et al., 2012). Events 4 and 8 demonstrate rapid swings of polarity during very short periods of time with a thickness of 0.3–0.5 m and may appear to be excursions; however, they are subjectively correlated to polarity subchrons of the GPTS in Ao et al. (2016). Event 5 is a long interval and could represent an actual geomagnetic event, however, it does not have to be a polarity chron, it might be an unresolved double excursion as reported in Kravchinsky (2017). Our correlation in Fig. 1 is based on the magnetostratigraphy profile in Anwar et al. (2015) where the age model is confirmed by resolution of the eccentricity cycles.

We conclude that the use of cyclostratigraphy in addition to magnetostratigraphy is the only correct approach to date red clay sequences when other dating methods are unavailable. However, this approach should be applied with caution, as incorrect data treatment can produce erroneous output for the spectral analysis. In any case, erroneous age models, which can result from visual

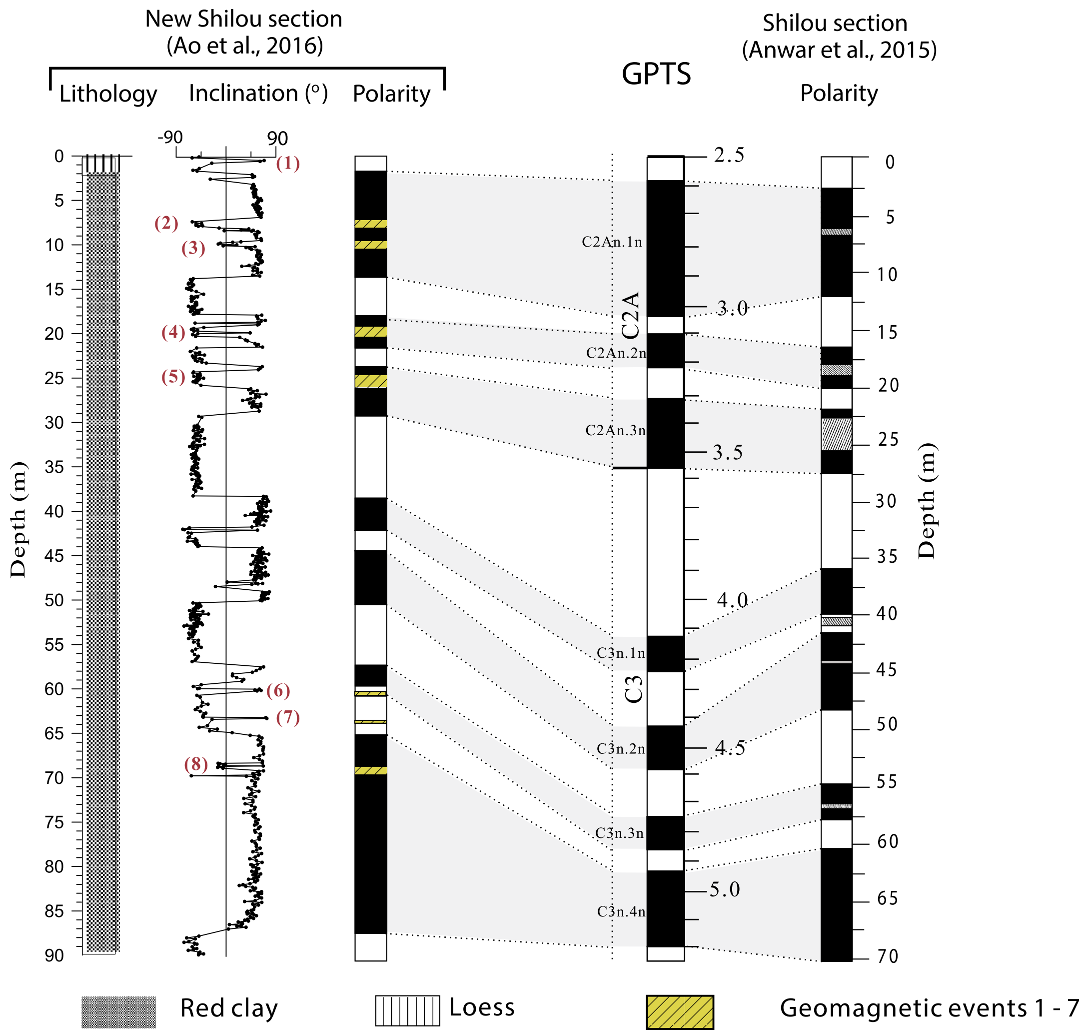

Fig. 1. Comparison of the Shilou Red Clay magnetostratigraphic records from Ao et al. (2016) and Anwar et al. (2015). The two sections situate ∼1 km from each other. Left panel – the magnetostratigraphic data from Ao et al. (2016), where possible short geomagnetic events (≤30 kyr) are marked with numbers from (1) to (7). Right panel is the age model based on tuning of magnetostratigraphy to cyclostratigraphy (Anwar et al., 2015). (For interpretation of the colors in the figure(s), the reader is referred to the web version of this article.)

correlation of polarity events in red clay and the GPTS, cause incorrect paleoclimate interpretations.

Acknowledgements

This work was financially supported by the National Natural Science Foundation of China (41772027, 41372037) and the Natural Sciences and Engineering Research Council of Canada (NSERC grant RGPIN-2014-04183).

Appendix A. Supplementary material

Supplementary material related to this article can be found online at https://doi.org/10.1016/j.epsl.2018.08.033.

References

Anwar, T., Kravchinsky, V.A., Zhang, R., 2015. Magneto- and cyclostratigraphy in the red clay sequence: new age model and apleoclimatic implication for the eastern Chinese Loess Plateau. J. Geophys. Res. 120, 6758–6770.

Ao, H., Roberts, A.P., Dekkers, M.J., Liu, X., Rohling, E.J., Shi, Z., An, Z., Zhao, X., 2016. Late Miocene–Pliocene Asian monsoon intensification linked to Antarctic ice-sheet growth. Earth Planet. Sci. Lett. 444, 75–87.

Ao, H., Dekkers, M.J., Roberts, A.P., Rohling, E.J., An, Z., Liu, X., Jiang, Z., Qiang, X., Xu, Y., Chang, H., 2017. Mineral magnetic record of the Miocene–Pliocene climate transition on the Chinese Loess Plateau, North China. Quat. Res. 88, 1–10.

Cande, S.C., Kent, D.V., 1992. Ultrahigh resolution marine magnetic anomaly profiles: a record of continuous paleointensity variations? J. Geophys. Res. 97 (B11), 15,075–15,083.

Cande, S.C., Kent, D.V., 1995. Revised calibration of the geomagnetic polarity timescale for the Late Cretaceous and Cenozoic. J. Geophys. Res. 100, 6093–6095.

Ding, Z., Yu, Z., Rutter, N.W., 1994. Towards an orbital time scale for Chinese loess deposits. Quat. Sci. Rev. 13, 39–70.

Ding, Z., Rutter, N., Sun, J., Yang, S., Liu, T., 2000. Re-arrangement of atmospheric circulation at about 2.6 Ma over northern China: evidence from grain size records of loess-palaeosol and red clay sequences. Quat. Sci. Rev. 19, 547–558.

Evans, M.E., Rutter, N., Ding, Z., 1991. Preliminary of magnetostratigraphy of the Red clay underlying the loess sequence at Baoji, China. Geophys. Res. Lett. 18, 1409–1412.

Gee, J.S., Kent, D.V., 2007. Source of oceanic magnetic anomalies and the geomagnetic polarity time scale. In: Schubert, G. (Ed.), Treatise on Geophysics, vol. 5: Geomagnetism. Elsevier, Amsterdam, pp. 455–507.

Jin, C., Liu, Q., Larrasoaña, J.C., 2012. A precursor to the Matuyama–Brunhes reversal in Chinese loess and its palaeomagnetic and stratigraphic significance. Geophys. J. Int. 190 (2), 829–842.

Kravchinsky, V.A., 2017. Magnetostratigraphy of the Lake Baikal sediments: a unique record of 8.4 Ma of continuous sedimentation in the continental environment. Glob. Planet. Change 152, 209–226.

Nie, J.S., 2011. Coupled 100-kyr cycles between 3 and 1 Ma in the terrestrial and marine paleoclimatic records. Geochem. Geophys. Geosyst. 12. https://doi.org/10.1029/2011GC003772.

Ogg, J.G., 2012. Geomagnetic polarity time scale. In: Gradstein, F.M., Ogg, J.G., Schmitz, M.D., Ogg, G.M. (Eds.), The Geologic Time Scale 2012. Elsevier B.V., pp. 85–113.

Ohno, M., Hayashi, T., Komatsu, F., Murakami, F., Zhao, M., Guyodo, Y., Acton, G., Evans, H.F., Kanamatsu, T., 2012. A detailed paleomagnetic record between 2.1 and 2.75 Ma at IODP Site U1314 in the North Atlantic: geomagnetic excursions and the Gauss–Matuyama transition. Geochem. Geophys. Geosyst. 13, Q12Z39. https://doi.org/10.1029/2012GC004080.

Spassov, S., Hus, J., Heller, F., Evans, M.E., Yue, L., von Dobeneck, T., 2011. The termination of the Olduvai Subchron at Lingtai, Chinese Loess Plateau: geomagnetic field behavior or complex remanence acquisition? In: The Earth's Magnetic Interior. Springer, Netherlands, pp. 235–245.

Sun, Y.B., Clemens, S.C., An, Z.S., Yu, Z.W., 2006. Astronomical timescale and palaeoclimatic implication of stacked 3.6-Myr monsoon records from the Chinese Loess Plateau. Quat. Sci. Rev. 25, 33–48.

Sun, Y.B., An, Z.S., Clemens, S., Bloemendal, J., Vandenberghe, J., 2010. Seven million years of wind and precipitation variability on the Chinese Loess Plateau. Earth Planet. Sci. Lett. 297, 525–535.

Vandenberghe, J.F., Lu, H.Y., Sun, D.H., Van Huissteden, J., Konert, M., 2004. The late Miocene and Pliocene climate in East Asia as recorded by grain size and magnetic susceptibility of the red clay deposits [Chinese Loess Plateau]. Palaeogeogr. Palaeoclimatol. Palaeoecol. 204, 239–255.

Xu, Y., Yue, L.P., Li, J.X., Sun, L., Sun, B., Zhang, J.Y., Ma, J., Wang, J.Q., 2009. An 11-Ma-old red clay sequence on the Eastern Chinese Loess Plateau. Palaeogeogr. Palaeoclimatol. Palaeoecol. 284, 383–391.

Xu, Y., Yue, L.P., Li, J.X., Sun, L., Sun, B., Zhang, J.Y., Ma, J., Wang, J.Q., 2012. Red clay deposits on the Chinese Loess Plateau during 11.0–2.6 Ma and its implications for long-term evolution of East Asian monsoon. Environ. Earth Sci. 66, 2021–2030.

Zhu, R., Zhang, R., Deng, C., 2007. Are Chinese loess deposits essentially continuous? Geophys. Res. Lett. 34, L17306. https://doi.org/10.1029/2007GL030591.

Supplementary Materials

Comment on “Late Miocene-Pliocene Asian monsoon intensification linked to Antarctic ice-sheet growth” [Earth Planet. Sci. Lett. 42 (2016) 75–87]

Rui Zhang[a,b,c], Vadim A. Kravchinsky[a,b,*], Taslima Anwar[b], Leping Yue[a,c], Jianxing Li[c,a], Jin Jiao[a]

a. *Institute of Cenozoic Geology and Environment, State Key Laboratory of Continental Dynamics, Department of Geology, Northwest University, Xi'an 710069, China*

b. *Geophysics, Department of Physics, University of Alberta, Edmonton, Alberta T6G 2E1, Canada*

c. *Xi’an Center of Geological Survey, China Geological Survey, Xi’an 710054, China*

* *Corresponding author e-mail: vadim@ualberta.ca; Tel: +86-18991191979; Fax: +86-29-88302202*

Earth and Planetary Science Letters

2018

Supplementary Table 1. Thicknesses and sedimentation rates of the red clay and classical loess sequences in China. Numbers of the sections correspond to Supplementary Figure 1.

Red clay section		Age of red clay sequence	Magnetostratigraphy and cyclostratigraphy dating	Thickness of red clay （m）	Sedimentation rate of red clay (mm/kyr)	Thickness of loess (m)	Sedimentation rate of loess (mm/kyr)	References
Central part of the Chinese Loess Plateau								
1	Lingtai	2.6-7.1Ma	yes	135	~29	130	~50	Ding et al., 1998
2	Chaona	2.6-8.1Ma	yes	125	~23	175	~67	Song et al., 2007; Nie et al., 2008
3	Pingliang	2.6-7.2Ma	no	130	~28	162	~62	Sun et al., 1998
4	Xunyi	2.6-6.8Ma	no	90	~22	140	~54	Xue et al., 2001
5	Jingchuan	2.6-7.7 Ma	no	126	~25	199	~75	Ding et al., 2001
6	Baoji	2.5-3.3Ma	yes	27	~14	160	~61	Evans et al., 1991
7	BJZ	2.6-6.9Ma	no	66	~15	–	–	An et al., 2001
8	ZJC	2.6-7.2Ma	no	57	~12	–	–	An et al., 2001
9	Xifeng	2.6-6.3Ma	no	60	~16	180	~69	Vandenberghe et al., 2004
10	Lantian	2.6-7.3Ma	no	60	~13	132	~50	Zheng et al., 1991

Eastern part of the Chinese Loess Plateau								
11	Baode	2.6-6.2Ma	no	73	~20	–	–	Zhu et al., 2008
12	Jiaxian	2.6-5.2Ma	no	65	~25	–	–	Ding et al., 1998
12	Jiaxian	2.6-8.1Ma	no	60	~11	–	–	Qiang et al., 2004
13	Weijiawa	4.2-8.1Ma	no	102	~21	–	–	Li et al., 2009
14	Shilou	2.6-11Ma	no	68	~8	–	–	Xu et al., 2009, 2012
14	Shilou	2.6-5.2Ma	yes	68	~26	–	–	Anwar et al., 2015
14	New Shilou	2.6-8.1Ma	no	88	~16	–	–	Ao et al., 2016
14	Newer Shilou	3.5-7.5Ma	no	68	~17	–	–	Ao et al., 2017

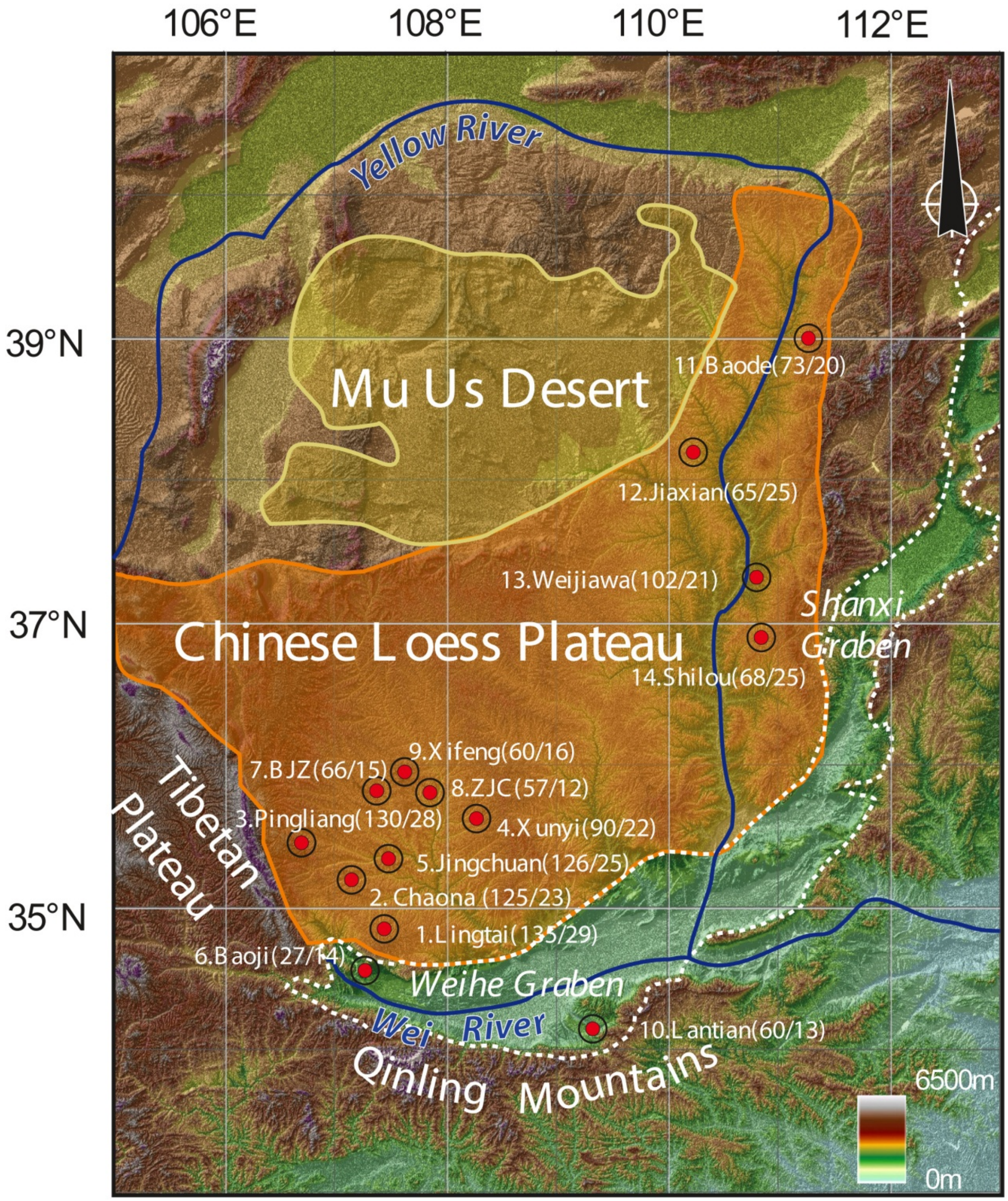

Supplementary Figure 1. Schematic map of the Chinese Loess Plateau with the red clay sections discussed in the text. Numbers of the sections correspond to Supplementary Table 1; numbers in the brackets are the thickness / average sedimentation rate (see Supplementary Table 1 for details).

References

An, Z., Kutzbach, J.E., Prell, W.L., Porter, S.C., 2001. Evolution of Asian monsoons and phased uplift of the Himalayan Tibetan plateau since Late Miocene times. Nature 411, 62–66.

Anwar, T., Kravchinsky, V.A., Zhang, R., 2015. Magneto- and cyclostratigraphy in the red clay sequence: New age model and paleoclimatic implication for the eastern Chinese Loess Plateau. J. Geophys. Res. Solid Earth 120, 6758–6770.

Ao, H., Roberts, A.P., Dekkers, M.J., Liu, X., Rohling, E.J., Shi, Z., An, Z., Zhao, X., 2016. Late Miocene-Pliocene Asian monsoon intensification linked to Antarctic ice-sheet growth. Earth Planet. Sci. Lett. 444, 75–87.

Ao, H. Dekkers, M.J., Roberts, A. P., Rohling, E. J., An, Z., Liu, X., Jiang, Z., Qiang, X., Xu, Y., Chang., H., 2017. Mineral magnetic record of the Miocene-Pliocene climate transition on the Chinese Loess Plateau, North China. Quat. Res. 88, 1–10. doi:10.1017/qua.2017.77

Ding, Z., Sun, J., Yang, S., Liu, T., 1998. Preliminary magnetostratigraphy of a thick eolian red clay-loess sequence at Lingtai, the Chinese Loess Plateau. Geophys. Res. Lett. 25, 1225–1228.

Ding, Z., Yang,S., Hou, S., 2001. Magnetostratigraphy and sedimentology of the Jingchuan red clay section and correlation of the Tertiary aeolian red clay sediments of the Chinese Loess Plateau. J. Geophys. Res. 106, 6399–6407.

Evans, M.E., Rutter, N., Ding, Z., 1991. Preliminary of magnetostratigraphy of the Red clay underlying the loess sequence at Baoji, China. Geophys. Res. Lett. 18, 1409–1412.

Li, J., Yue, L., Xu, Y., 2009.Discovery and Geological Significance of Red Clay in the

Liulin Section in the West Part of Lüliang Mountains. Acta Sedimentologica Sinica 27, 1184–1190. In Chinese.

Nie, J., 2011. Coupled 100-kyr cycles between 3 and 1 Ma in the terrestrial and marine paleoclimatic records. Geochemis. Geophys. Geosys. 12, doi:10.1029/2011GC003772, http://dx.doi.org/ 10.1029/2007GL031430.

Qiang, X., Li, Z., Powell, C.M., Zheng, H., 2001. Magnetostratigraphic record of the Late Miocene onset of the East Asian monsoon, and Pliocene uplift of north-ern Tibet. Earth Planet. Sci. Lett. 187, 83–93.

Song, Y., Fang, X., Torii, M., Ishikawa, N., Li, J., An, Z., 2007. Late Neogene rock magnetic record of climatic variation from Chinese eolian sediments related to the uplift of the Tibetan Plateau. J. Asian Earth Sci. 30, 324–332.

Sun, D., Shaw, J., An, Z., Cheng, M., Yue, L., 1998. Magnetostratigraphy and paleoclimatic interpretation of a continuous 7.2Ma Late Cenozoic eolian sediments from the Chinese Loess Plateau. Geophys. Res. Lett. 25, 85–88.

Sun, Y., Clemens, S.C., An, Z., Yu, Z., 2006. Astronomical timescale and palaeoclimatic implication of stacked 3.6-Myr monsoon records from the Chinese Loess Plateau. Quat. Sci. Rev. 25, 33–48.

Sun, Y., An, Z., Clemens, S., Bloemendal, J., Vandenberghe, J., 2010. Seven million years of wind and precipitation variability on the Chinese Loess Plateau. Earth Planet. Sci. Lett. 297, 525–535.

Vandenberghe, J.F., Lu, H., Sun, D., van Huissteden, J., Konert, M., 2004. The late Miocene and Pliocene climate in East Asia as recorded by grain size and magnetic susceptibility of the Red Clay deposits [Chinese Loess Plateau]. Palaeogeogr. Palaeoclimatol. Palaeoecol. 204, 239–255.

Xu, Y., Yue, L., Li, J., Sun, L., Sun, B., Zhang, J., Ma, J., Wang, J., 2009. An 11-Ma-old red clay sequence on the Eastern Chinese Loess Plateau. Palaeogeogr. Palaeoclimatol. Palaeoecol. 284, 383–391.

Xu, Y., Yue, L., Li, J., Sun, L., Sun, B., Zhang, J., Ma, J., Wang, J., 2012. Red clay deposits on the Chinese Loess Plateau during 11.0–2.6 Ma and its implications for long-term evolution of East Asian monsoon. Environ. Earth Sci. 66, 2021–2030.

Xue, X., Yue. L., Wang. J., 2001. Boundary between Neogene and Quaternary from a profile upper Cenozoic group in Xunyi of Shanxi. Journal of Stratigraphy (in Chinese). 25, 161-165.

Zheng, H., An, Z., Shaw, J., 1992. New contribution to Chinese Plio- Pleistocene magnetostratigraphy. Phys. Earth Planet. Int. 70, 146-153.

Zhu, Y., Zhou, L., Mo, D., Kaakinen, A., Zhang, Z., Fortelius, M., 2008. A new magnetostratigraphic framework for late Neogene Hipparion Red Clay in the eastern Loess Plateau of China. Palaeogeogr. Palaeoclimatol. Palaeoecol. 268, 47–57.